View Article Online / Journal Homepage / Table of Contents for this issue
Dynamic Article Links

CrystEngComm

Cite this: *CrystEngComm*, 2012, **14**, 4486–4489

www.rsc.org/crystengcomm

PAPER

Improvement of defect reduction in semi-polar GaN grown on shallow-trenched Si(001) substrate

Ling Lee,*[a] Kun-Feng Chien,[a] Wu-Ching Chou,*[a] Chih-Hsin Ko,[b] Cheng-Hsien Wu,[b] You-Ru Lin,[b] Cheng-Tien Wan,[b] Clement H. Wann,[b] Chao-Wei Hsu,[c] Yung-Feng Chen[c] and Yan-Kuin Su[c]

Received 8th March 2012, Accepted 19th April 2012
DOI: 10.1039/c2ce25335f

Published on 16 May 2012. Downloaded by National Chiao Tung University on 28/04/2014 23:13:11.

The improved design of sub-micron trenches on Si(001) substrate was demonstrated for defect suppression in semi-polar selectively-grown GaN layers. Cathodoluminescence and transmission electron microscopy measurements revealed a dramatically decreased density of threading dislocations and stacking faults near the surface of the overgrown GaN layer when the trench width ranged from 500 to 1500 nm. It was observed that defects were effectively trapped inside the trench when the ratio of trench depth to the SiO_2 thickness is less than 0.66. In addition, a significant reduction of intrinsic polarization electric field was achieved for the InGaN/GaN multiple quantum well on the GaN selectively grown from the Si trenches.

Introduction

III-nitrides become the material chosen for the solid-state lighting recently. However, the commonly used c-plane sapphire substrate raises an important problem of strong intrinsic polarization electric field which separates electrons and holes in multiple quantum well (MQW) active layers and reduces emission efficiency. Since 2000, semi-polar and non-polar GaN were designed to solve this difficulty by applying alternative substrates such as $LiAlO_2$(001), a-plane SiC, Si(001), r-plane and m-plane sapphires substrates.[1,2] Among them, Si(001) substrates attract increasing attention because overgrown GaN layers exhibit semi-polar characteristics and low-cost Si wafers benefit the large-scale production. Nevertheless, the developments of these semi-polar and non-polar GaN so far are not very successful. High densities of structural defects, including threading dislocations and stacking faults,[3–5] were found and degraded the device performance.[6] For GaN grown on Si(001) substrate, an approach has been utilized to reduce the defect density by opening V-grooved trenches with thin SiO_2 masks, and then selectively overgrowing the GaN layers in trenches.[2,7,8] Whereas transmission electron microscopy (TEM) analyses have revealed the suppression of dislocation density, many dislocations with a density of larger than 10^8 cm^{-2} remain at the GaN surface, especially above the masked regions. In this study, an improved design of the shallow trench on Si(001) substrate was demonstrated. Investigations of cathodoluminescence (CL) show that the density of structural defects can be significantly reduced using shallow trenches with width ranges from 500 to 1500 nm. The dependence of the effective reduction of defects on the depth of trenches for a particular SiO_2 mask thickness was investigated. Additionally, the emission peak energies of CL and photoluminescence (PL) detected from the InGaN/GaN MQW, which were grown on the selectively grown GaN, show less dependence on the excitation power. It implies that the selectively grown GaN layers exhibit semi-polar characteristics and is very important in InGaN/GaN MQW-based solid-state light emitting devices for their improved emission efficiency.

Experimental details

The specimen preparation began with a 250-nm-thick SiO_2 mask layer that was deposited on a Si(001) wafer. Trenches along the [1$\bar{1}$0] direction with widths ranging between 200 and 2000 nm were fabricated using 193 nm immersion lithography and reactive ion etching. Then, the wafer underwent anisotropic KOH etching to form Si(111) facets. The cross-section of a single trench is trapezoid, with two inclined sidewalls of Si(111) surfaces and a Si(001) surface at the bottom. To ensure selective growth and dislocation trapping, the wafer was not immersed in HF solution before growth and the SiO_2 masks above the sidewalls of the trenches were preserved. The GaN layer was grown using a commercial metal–organic chemical vapor deposition system at 70 Torr and 1150 °C after a thin nucleation the AlN layer was grown at the same temperature. GaN layers that were grown on a planar Si substrate and a c-plane sapphire substrate under the same growth conditions were used as reference samples. To verify the semi-polar characteristics, five pairs of $In_{0.06}Ga_{0.94}N$/GaN MQW with a well width of 3 nm were deposited on top of the GaN layer grown on the patterned

[a]*Department of Electrophysics, National Chiao Tung University, Hsinchu 300, Taiwan, Republic of China. E-mail: wurtzite@xuite.net; wuchingchou@mail.nctu.edu.tw*
[b]*Taiwan Semiconductor Manufacturing Co., Ltd, Hsinchu 300, Taiwan, Republic of China*
[c]*Institute of Microelectronics and Advanced Optoelectronic Technology center, National Cheng Kung University, Tainan 701, Taiwan, Republic of China*

This journal is © The Royal Society of Chemistry 2012

View Article Online

Published on 16 May 2012. Downloaded by National Chiao Tung University on 28/04/2014 23:13:11.

Si substrate and also grown on c-plane sapphire for comparison. The structural characteristics of these specimens were analyzed by both TEM and CL. The former was performed using an FEI Tecnai G2 F20 microscope at 200 kV and room temperature. The latter was performed using a JEOL JSM-7001F scanning electron microscope at 15 kV and a low temperature of 15 K. The luminescence signals were analyzed by a Horiba Jobin-Yvon iHR550 0.5 m monochromator and detected using a liquid-nitrogen-cooled charge-coupled device (CCD) with an energy resolution of 0.3 meV.

Results and discussions

The morphologies of the GaN layers that were grown from trenches were measured by scanning electron microscopy (SEM). Fig. 1(a) and (b) show the cross-sectional SEM images of GaN that was grown from a 1000-nm-wide and a 2000-nm-wide trench, respectively, with the trench depth of 150 nm. Fig. 1(a) shows the selective growth of the GaN(0001) c-plane from the two opposite Si{111} planes at the sidewalls of the trench and along the [111] direction. The GaN growth from both Si(111) inclined sidewalls is much faster than that from the bottom Si(001) plane. GaN grown from both sidewalls merges and stops the growth of GaN from the bottom Si(001) plane. As a result, a void exists at the center of the bottom Si(001) plane. The GaN[0001] axis was parallel to Si[111] and the GaN [1$\bar{1}$01] axis was parallel to Si[001], as indicated by the arrows in Fig. 1(a). Owing to the selective growth, GaN with a (1$\bar{1}$01) semi-polar surface can be successfully grown by utilizing a shallow-trenched Si(001) wafer. However, the selective growth of GaN from a 2000-nm-wide trench, as shown in Fig. 1(b), was poor. GaN grew along Si[001] from the bottom of a wide shallow-trench and also grew along Si[111] from the sidewalls. Therefore, no void was observed at the center of the 2000-nm-wide trench.

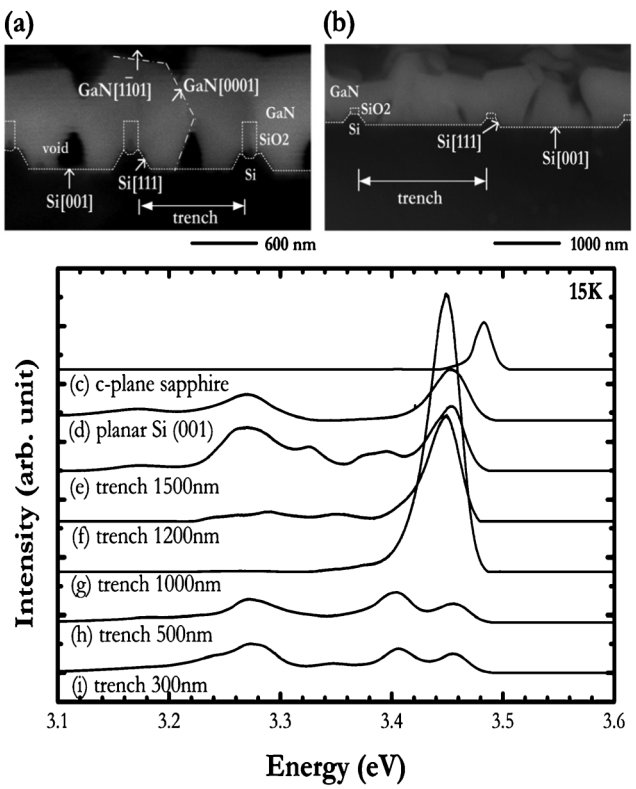

Fig. 1 Cross-sectional scanning electron microscopy images of GaN grown on (a) 1000-nm-wide and (b) 2000-nm-wide trenched Si (001) wafer. 15 K CL spectra of GaN grown on (c) c-plane sapphire, (d) planar Si(001), and trenches (e) to (i).

The improved structural quality in the selectively-grown semi-polar GaN layer was demonstrated in accordance to CL spectra measured at 15 K, as shown in Fig. 1(c) to 1(i). Fig. 1(c) shows, as a reference, an emission peak at 3.48 eV without shoulders for a GaN epilayer grown on a c-plane sapphire. The peak is close to the transition of the excitons bound to native neutral donors (DX) in an undoped GaN epilayer at 3.476 eV.[9] Fig. 1(d) and 1(e) show a broader emission peak at 3.45 eV for GaN that was grown on a planar Si(001) wafer and on the 1500-nm-wide trench. The red-shift is caused by the tensile strain that is induced by the mismatch between the thermal expansion coefficients of GaN and Si. Additional peaks were observed at 3.27, 3.32, and 3.40 eV. Previous studies of non-polar and semi-polar GaN epilayers have attributed these peaks at 3.27, 3.32, and 3.40 eV to the emissions from partial dislocations terminating the basal plane faults, prismatic-plane stacking faults, and basal plane stacking faults, respectively.[10] The similar lineshape observed in Fig. 1(d) and 1(e) shows that a high density of structural defects occur in GaN grown in trenches wider than 1500 nm.

As the width of the trench was reduced to 1200 nm, as shown in Fig. 1(f), the emissions that were associated with these structural defects, especially dislocations, became weaker and the DX emission increased. It implies that the selective growth succeeds in the inhibiting of dislocations generated from Si(001).[11] Based on the emission intensity of DX, the optimized trench width was 1000 nm, as shown in Fig. 1(g). In that figure, the intensities associated to dislocations are less than 0.01 times of the DX emission intensity. This result is superior to that for an a-plane GaN epilayer grown on an AlGaN buffered r-plane sapphire,[5] which yields strong emissions attributed to stacking faults and dislocations and a relatively weak DX emission. However, if the width of the trench was further reduced down to less than 500 nm, then the relative intensity associated with both dislocation and stacking faults increased, as shown in Fig. 1(h) and 1(i). Therefore, for a trench depth of 150 nm and a mask thickness of 250 nm, the optimal trench width for growing high-quality and semi-polar GaN on Si(001) is 1000 nm. Our design is better than that demonstrated by Hikosaka *et al.*, whose semi-polar GaN was grown on V-grooves with width and depth of 1000 and 700 nm, respectively, and a 70 nm-thick SiO_2 mask.[12] In their studies, the intensity of the peak at 3.27 eV from GaN that was grown above the groove and below the mask was associated with dislocations and was around 0.7 times the intensity of the DX emission. For GaN above the mask region the dislocation-related emission was even stronger than the DX emission.

In order to discover the dependence of dislocation density on the mask thickness and width/depth of the trench, Fig. 2(a) and 2(b) schematically depict the structures of trenches with a fixed trench width of 1000 nm and a mask thickness of 250 nm, but with depths of 150 nm and 450 nm, respectively. In Fig. 2(c), the trench depth equals that in Fig. 2(a), but the trench width is 200 nm. Dashed lines represent the threading dislocations. The

View Article Online

Published on 16 May 2012. Downloaded by National Chiao Tung University on 28/04/2014 23:13:11.

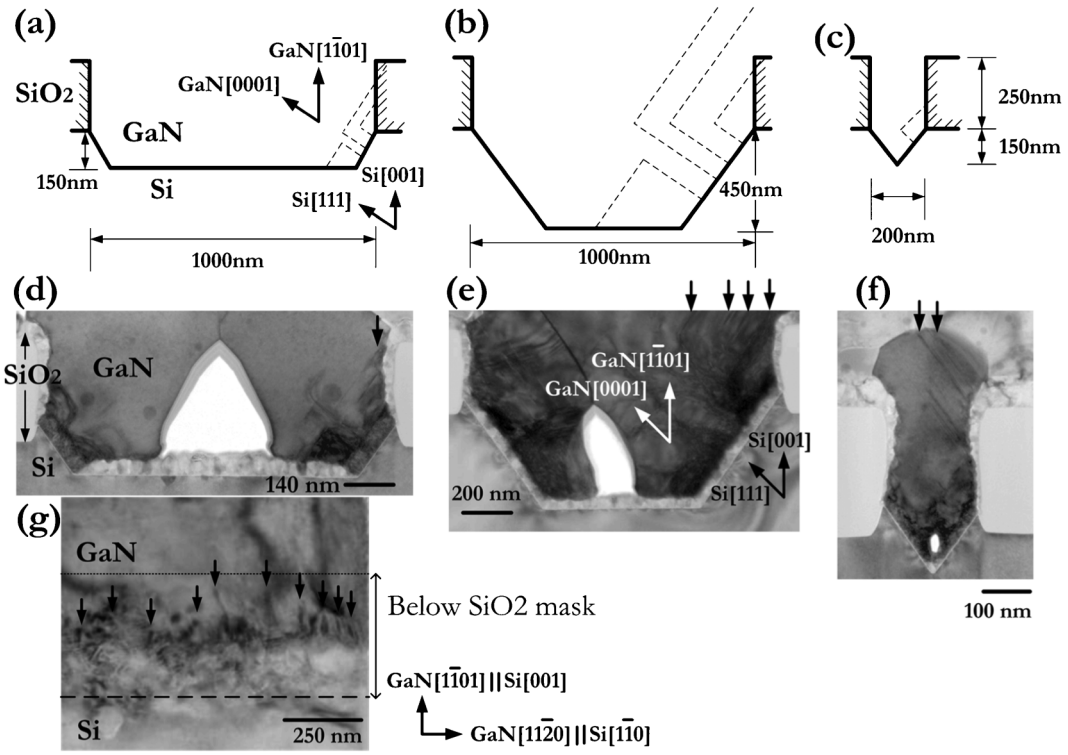

Fig. 2 Schematic plots of the propagation of dislocations at trenches with (a) width of 1000 nm and depth of 150 nm, (b) width of 1000 nm and depth of 450 nm, and (c) width of 200 nm and depth of 150 nm. Cross-sectional TEM images of (d) and (g) correspond to (a), while (e) and (f) correspond to (b) and (c), respectively.

propagation of threading dislocations, which satisfies the condition for minimized total energy, starts from the Si{111} sidewalls along the GaN[0001] axis, and bends to become parallel to the c-plane along the [1$\bar{1}$00] axis.[13] For the 150 nm-deep trench, as shown in Fig. 2(a), the SiO_2 mask is relatively thick, and almost all the upwardly bent threading dislocations can be trapped by sidewalls before they reach the surface. However, in the case of the 450-nm-deep trench, the upwardly bent threading dislocation could not be effectively trapped. As a result, according to Fig. 2(a), the highest ratio of trench depth to the SiO_2 mask thickness for effectively trapping of dislocations is 0.66. This result implies that the largest depth of trench that can adequately trap the dislocations is 166 nm when the 250 nm-thick SiO_2 mask is used. To confirm this prediction, Fig. 2(d) to 2(f) show the cross-sectional bright-field TEM images, taken as the electron beam incident along the $[11\bar{2}0]_{GaN}//[1\bar{1}0]_{Si}$ direction, of GaN grown in trenches as Fig. 2(a) to 2(c), respectively. Dark lines and arrows indicate threading dislocations in GaN selectively grown from both the Si{111} sidwalls. Fig. 2(d) illustrates that the shallow trench herein trapped almost all the threading dislocations. On the contrary, threading dislocations propagate to the GaN surface when the trench is deeper, as shown in Fig. 2(e), which presents the same results as found elsewhere.[7,8] The reduction of threading dislocation density near surface was also evaluated by the cross-sectional bright-field TEM image of the 150-nm-deep trench that was cleft along the long trench axis as shown in Fig. 2(g). Threading dislocations indicated by black arrows stop below the top surface of the SiO_2 masks. According to Fig. 2(d) and 2(g), this selective growth approach can yield a dislocation density of less than 1×10^8 cm^{-2} at the upper half of the GaN layer. It explains why the 1000-nm-wide and 150-nm-deep trench significantly suppresses the dislocation-related CL intensity, as shown in Fig. 1(g). The trench in Fig. 2(c) has the same trench depth as in Fig. 2(a) but its width is only 200 nm. The selective growth is not as good as in Fig. 2(d), and dislocations emerge from the Si(111) plane as well as from the SiO_2 mask, as shown in Fig. 2(f). This result qualitatively illustrates that the defect-related emission of the CL spectra becomes stronger as the width of the trench is reduced to less than 500 nm, as shown in Fig. 1(h) and 1(i).

The selective growth of GaN from a Si trench not only benefits the suppression of dislocations but also provides a semi-polar GaN top layer. The semi-polar GaN top layer serves as a template for the $In_{0.06}Ga_{0.94}N$/GaN MQW, reducing the intrinsic polarization electric field and thereby increases the emission efficiency of the MQW. Five pairs of low-In-content $In_{0.06}Ga_{0.94}N$/GaN MQW with a well width of 3 nm were deposited on patterned Si with a trench width of 1000 nm and on a GaN template with substrate of c-plane sapphire as a reference. At such low indium content, the electric field induced quantum confined stark effect (QCSE) dominated the carrier recombination, while the effects on carrier localization are minor.[14] This study concentrated on the power-dependent PL and CL at low temperature to screen the QCSE effect and investigate the built-in electric field strength. Fig. 3 shows the emission energies of $In_{0.06}Ga_{0.94}N$/GaN MQW under different excitation power densities. PL measurements of the MQW that was grown on a c-plane GaN template revealed an increase in peak energy from

 This journal is © The Royal Society of Chemistry 2012

View Article Online

Published on 16 May 2012. Downloaded by National Chiao Tung University on 28/04/2014 23:13:11.

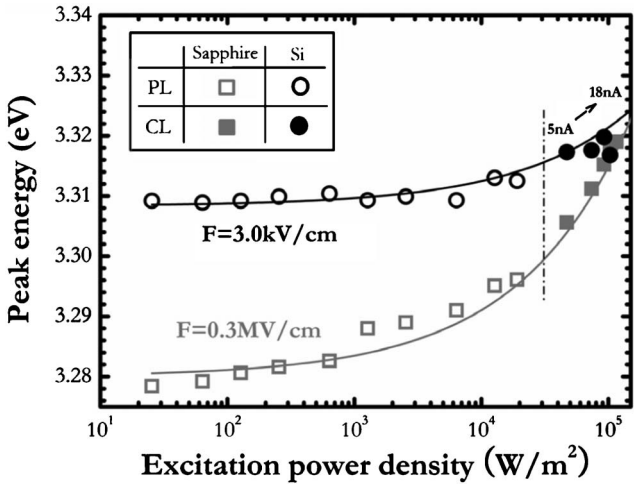

Fig. 3 The corresponding peak energies at different excitation power densities by PL and probe currents by CL of InGaN/GaN MQW grown on c-plane sapphire and patterned Si(001) substrate, respectively.

3.279 to 3.295 eV as the laser excitation increased from 20 to 2×10^4 W m^{-2}. The blue-shift of energies that corresponds to the increase in excitation power was fitted by a theoretical model,[15] as plotted by the solid curve, for an built-in electric field strength of 0.3 MV cm^{-1}. The field strength is close to the calculated value in a low-In-content MQW.[16] The CL measurements revealed the screening of the QCSE at the higher-level injection. An increase in peak energy from 3.302 to 3.320 eV as the probe current of the focused electron beam increased from 5 to 18 nA. Since the increasing of peak energies observed by CL lays on the simulated curve, we proposed that CL probe currents of 5 and 18 nA are equivalent to a PL optical excitation of power density of 2×10^4 and 11×10^4 W m^{-2}. On the contrary, for the specimen grown on patterned Si substrate the intensity of MQW increases more than an order of magnitude and the observed energy shift from MQW on patterned Si substrate decreases from 41 meV to 10 meV under low excitation conditions. It corresponds to an electric field strength of 3.0 kV cm^{-1}, which approaches the value observed elsewhere in the MQW on the *m*-plane GaN.[17]

Conclusions

In conclusion, the improved design of trenched Si(001) substrate was demonstrated to suppress defects in overgrown semi-polar GaN. CL and TEM revealed that effective trapping of threading dislocation and stacking fault in the trench succeeds when the trench width was between 500 and 1500 nm and the ratio of the trench depth to the SiO_2 sidewall thickness was less than 0.66. In this work, a threading dislocation of less than 1×10^8 cm^{-2} and negligible emissions associated with stacking faults were achieved. In addition, the intrinsic polarization electric field in InGaN/GaN MQW grown on GaN that has been selectively grown from the Si trenches was markedly reduced.

Acknowledgements

This work was supported by the National Science Council under grant No. NSC 100-2119-M-009-003 and No. NSC 100-2731-M-009-001-NPI, Ministry of Education under grant number MOE-ATU 99W957, Center for interdisciplinary science of National Chiao Tung University, and Taiwan Semiconductor Manufacturing Co., Ltd.

References

1 B. A. Haskell, S. Nakamura, S. P. DenBaars and J. S. Speck, *Phys. Status Solidi B*, 2007, **244**, 2847.
2 C. H. Chiu, D. W. Lin, C. C. Lin, Z. Y. Li, W. T. Chang, H. W. Hsu, H. C. Kuo, T. C. Lu, S. C. Wang, W. T. Liao, T. Tanikawa, Y. Honda, M. Yamaguchi and N. Sawaki, *Appl. Phys. Express*, 2011, **4**, 012105.
3 I. Lo, C. H. Hsieh, Y. L. Chen, W. Y. Pang, Y. C. Hsu, J. C. Chiang, M. C. Chou, J. K. Tsai and D. M. Schaadt, *Appl. Phys. Lett.*, 2008, **92**, 202106.
4 B. Bastek, F. Bertram, J. Christen, T. Wernicke, M. Weyers and M. Kneissl, *Appl. Phys. Lett.*, 2008, **92**, 212111.
5 Z. H. Wu, A. M. Fischer, F. A. Ponce, T. Yokogawa, S. Yoshida and R. Kato, *Appl. Phys. Lett.*, 2008, **93**, 011901.
6 M. F. Schubert, S. Chhajed, J. K. Kim, E. F. Schubert, D. D. Koleske, M. H. Crawford, S. R. Lee, A. J. Fischer, G. Thaler and M. A. Banas, *Appl. Phys. Lett.*, 2007, **91**, 231114.
7 S. Tanaka, Y. Honda, N. Kameshiro, R. Iwasaki, N. Sawaki and T. Tanji, *Jpn. J. Appl. Phys.*, 2002, **41**, L846.
8 G. T. Chen, S. P. Chang, J. I. Chyi and M. N. Chang, *Appl. Phys. Lett.*, 2008, **92**, 241904.
9 G. D. Chen, M. Smith, J. Y. Lin, H. X. Jiang, S. H. Wei, M. A. Khan and C. J. Sun, *Appl. Phys. Lett.*, 1996, **68**, 2784.
10 R. Liu, A. Bell, F. A. Ponce, C. Q. Chen, J. W. Yang and M. A. Khan, *Appl. Phys. Lett.*, 2005, **86**, 021908.
11 S. Joblot, E. Feltin, E. Beraudo, P. Vennéguès, M. Leroux, F. Omnès, M. Laügt and Y. Cordier, *J. Cryst. Growth*, 2005, **280**, 44.
12 T. Hikosaka, T. Narita, Y. Honda, M. Yamaguchi and N. Sawaki, *Appl. Phys. Lett.*, 2004, **84**, 4717.
13 A. Sakai, H. Sunakawa and A. Usui, *Appl. Phys. Lett.*, 1997, **71**, 2259.
14 S. Chichibu, T. Sota, K. Wada and S. Nakamura, *J. Vac. Sci. Technol., B*, 1998, **16**, 2204.
15 E. Kuokstis, J. W. Yang, G. Simin, M. A. Khan, R. Gaska and M. S. Shur, *Appl. Phys. Lett.*, 2002, **80**, 977.
16 T. Takeuchi, S. Sota, M. Katsuragawa, M. Komori, H. Takeuchi, H. Amano and I. Asakaki, *Jpn. J. Appl. Phys.*, 1997, **36**, L382.
17 T. Takeuchi, H. Amano and I. Akasaki, *Jpn. J. Appl. Phys.*, 2000, **39**, 413.